Chapter - 4

Apremilast loaded nanostructured lipid carriers

4. Introduction

Nanostructured lipid carriers (NLCs) are second-generation solid lipid nanocarriers with liquid lipid in the structure. The liquid lipid incorporation increases the imperfection in the solid particle, which enhances the drug entrapment, reduces drug leaching on storage, and alters the drug release. The small particle size of the NLCs forms a thin layer on the skin, leading to the occlusive layer, the occlusive layer inhibits the TEWL. The reduction in TEWL leads to hydration of the skin and increasing the gaps between corneocytes. NLCs protect the drug from degradation, skin retention and prolongs drug release within skin layers, which favors skin targeting and reduces the systemic adverse effects [1]. Literature showed a few studies for Apremilast-loaded NLCs, which showed that NLCs could be a suitable nanocarrier system for effective topical delivery of Apremilast. However, these studies were not explored extensively for ex-vivo and dermal pharmacokinetics. These designed nanocarriers showed particle sizes of more than 500 nm for topical delivery [2,3]. Particle size less than 200 nm is reported as most suitable to improve permeation in psoriasis conditions. The prolonged drug release from the NLCs formulation can provide the desired therapeutic efficacy with reduced dose and dosing frequency [4].

4.1. Materials

Precirol ATO 5 (glyceryl palmitostearate), Compritol 888 ATO (glyceryl dibehenate) were obtained as gift samples from Gattefosse India. Stearic acid, Glyceryl monostearate, and Oleic acid were purchased from Central Drug House (P) Ltd fine chemicals (New Delhi, India). Dynasan 114 (trimyristin) was acquired from Sasol Olefins & Surfactants (Germany). Polysorbate 80 was obtained from S. D. Fine Chemicals (India). Acetonitrile, Methanol (HPLC grade), orthophosphoric acid, methylparaben, propylparaben, and potassium dihydrogen phosphate were procured Merck, Mumbai, India. Antibiotic-antimycotic solution and

Dulbecco's modified Eagle's medium (DMEM) were obtained from Thermofisher Scientific (India). Fetal bovine serum was purchased from Himedia (Mumbai, India). Kolliphor CS12, Carbopol® 974P NF and Lutrol® F 127 (Poloxamer 407) were received as a gift sample from Lubrizol (Belgium) and BASF (India), respectively. Cellophane tape was purchased from Scotch 3 M, USA. All other solvents, reagents, and chemicals used were of analytical grade.

4.2. Methods

4.2.1. Selection of lipids, surfactants and drug excipient compatibility study

The liquid lipid selection was performed by saturation solubility method, in which excess amount of Apremilast was added to 0.5 g individual oil (Labrafil M 1944 CS, Labrasol ALF, Miglyol 810, Miglyol 812, Labrafac CC, Labrafil M 2125 CS, and Myristol). The mixture was subjected to vortexing and placed on the orbital shaker for 24 h at room temperature. After 24 h, the samples were subjected to centrifugation to settle the undissolved drug, and the supernatant solution was collected. Appropriate dilutions were made, and the amount of Apremilast dissolved was analyzed using a validated analytical method [5]. The solid lipid and surfactant selection procedures are the same as mentioned in section 3.2.1. The drug excipient compatibility study was performed for liquid lipid as mentioned in section 3.2.2.

4.2.2. Quality by design approach

Identification of quality target product profile, critical quality attributes, risk assessment and design selection for optimization were performed as mentioned in section 3.2.3.

4.2.3. Preparation and optimization of nanostructured lipid carriers

The NLCs dispersion was prepared by emulsification followed by probe sonication technique [5]. The batch quantity of lipids (solid and liquid (75:25)), Apremilast and preservative agents (methylparaben and propylparaben) were transferred into a vial. Acetone was added to dissolve the content for homogeneous dispersion. The lipid mixture was heated at 70 ± 2 ºC for 30 min

to evaporate the acetone and to melt the lipid under constant stirring. The batch quantity surfactant was weighed in a separate vial, and the solution was prepared using Milli-Q water. The solution was subjected to heating at 70 ± 2 ºC. The hot aqueous solution was transferred into a lipid mixture and stirred continuously for 20 min to form the emulsion phase. The formed emulsion was probe sonicated and cooled to room temperature to solidify NLCs particles under continuous stirring for an additional 20 min [6]. The formulation was centrifuged at 5000 rpm for 5 min, and the supernatant lipid nanocarriers dispersion was subjected to ultracentrifugation at 35,000 rpm to separate the NLCs from dispersion. The supernatant was separated, and the settled nanocarriers were redispersed in milli-Q water.

4.2.4. Scale-up studies of the optimized formulation

From the validation parameters obtained from the design space, the scale-up of the optimized batch was performed up to 50 mL and 100 mL. The process parameter i.e. sonication time was varied within the design space. The scale-up batches were performed as mentioned in section 3.2.5.

4.2.5. Characterization of nanostructured lipid carriers dispersion

The Attenuated total reflection-Fourier transform infrared spectroscopy (ATR-FTIR), Particle size, zeta potential, morphology, entrapment efficiency, in-vitro drug release studies of NLCs dispersion, cytotoxicity study, cell uptake study using Coumarin-6, and quantitative real-time polymerase chain reaction (PCR) analysis for expression of TNF-α in psoriasis induced model, was performed as mentioned in section 3.2.6

4.2.6. Preparation and characterization of Apremilast loaded NLCs gel and free drug-loaded gel

Preparation and evaluation for rheological behavior, occlusive test, ex-vivo skin permeation studies, dermal retention studies, ex-vivo dermal distribution studies, dermatokinetic estimation were performed as mentioned in section 3.2.7 and section 3.2.8.

4.2.7. In-vivo studies

4.2.7.1. Skin retention and skin irritation study

The animal study was performed with prior approved protocols by the IAEC (Protocol No. IAEC/RES/24/06/Rev-1/28/28). The animals were treated with Apremilast loaded NLCs gel and free drug-loaded gel. Skin retention studies were performed as mentioned in section 3.2.9.2.

4.2.8. Storage stability of Apremilast loaded NLCs gel

The selected Apremilast loaded NLCs gel was evaluated for storage stability up to three months at 4 ℃ and 25 ℃. The gel was evaluated for particle size integrity (using Malvern Zetasizer) and the assay using the HPLC method [5].

4.2.9. Statistical analysis

The statistical analysis was performed for the data obtained from three individual experiments. GraphPad Prism 5.0 was utilized for statistical analysis. The mean of the two groups was compared using two-way ANOVA, and the value at $p < 0.05$ was considered statistically significant.

4.3. Results and discussion

4.3.1. Screening of lipids and surfactants

Lipids for the development of NLCs were selected based on the solubility of Apremilast in melted lipid. Apremilast exhibited the highest solubility in Precirol ATO5 (Precirol ATO5 >

Stearic acid > Comptriol 888 ATO > Dynasan 114 > Glyceryl monostearate) in solid lipids (as mentioned in Table 3.1) and Labrafil M 2125 (Labrafil M 2125 > Labrafil M 1944 > Oleic acid > Miglyol 810 > Myristol > Labrafac CC > Miglyol 812) compared to other liquid lipids as mentioned in **Table 4.1**. Thus, Precirol ATO5 was selected as the solid lipid, and Labrafil M 2125 was selected as a liquid lipid for NLCs preparation. The highest solubility favors maximum entrapment efficiency, increased drug loading and reduced drug expulsion. The reduced drug expulsion is expected due to the high interaction affinity of the drug towards lipids. Labrafil M 2125 (Linoleyl macrogol-6 glycerides) is a medium-chain triglyceride that exhibits nano-emulsification property, enhances the solubility and permeation of the drug upon topical application (skin) [7]. The Kolliphor CS12 was used as a surfactant, and it assisted in emulsification and reduced particle size by stabilizing the lipid-water interface. The drug excipient compatibility showed no significant change in the percent assay (< 1%) and physical appearance.

Table 4.1. The solubility of Apremilast in Liquid lipids

Lipid	**Apremilast solubility (µg/g)**
Miglyol 810	325.229 ± 1.020
Miglyol 812	262.744 ± 0.812
Oleic acid	370.654 ± 1.571
Labrafil M 2125	597.009 ± 2.790
Labrafil M 1944	425.653 ± 2.452
Labrafac CC	265.965 ± 0.852
Myristol	287.0159 ± 0.960

4.3.2. Quality by design

The identification of the QTPP initiated the QbD approach for the preparation of NLCs. Risk identification and risk assessment were performed using FMEA. Critical process parameters and critical material attributes were identified using the Ishikawa diagram, as mentioned in

section 3.3.4. The lipid amount and surfactant concentration (formulation variables) and sonication time (process variables) were considered for the optimization of NLCs dispersion.

4.3.3. Design of experiments for optimization

To study the effect of formulation and process variables on desired characteristics of finished formulation, DOE was implemented. Box-Behnken experimental design was employed with 17 trials (3 factors and 3 levels) using design-expert software (Design-Expert® 8.0, State-Ease Inc., Minneapolis, USA). The amount of lipid and surfactant concentration was selected as the material attributes, and sonication time was selected as the process parameter. Entrapment efficiency and particle size were selected as dependent variables as critical quality attributes of the designed formulation. For formulation optimization, the amount of lipid, surfactant concentration, and sonication time (Independent variables) was studied at low, medium, and high levels. The 17 batches obtained from the design were executed as summarized in **Table 4.2.** The experiments were performed by varying independent variables keeping all other parameters (process and formulation parameters) persistent. Response variables (dependent variables) were investigated in terms of particle size and entrapment efficiency. The preservatives methylparaben and propylparaben, were used in the concentrations of 0.2% w/v, and 0.02% w/v (1:10 ratio). The combination provided the synergistic activity and was constant in all trials. The obtained data were statistically evaluated using analysis of variance for the selected input factors model efficiency and significance.

4.3.3.1. Effect of independent variables on particle size

The average particle size of Apremilast loaded NLCs were in the range of 95.40 to 201.30 nm, as represented in **Table 4.2**. The coded values of selected independent variables are represented as regression equation 4.1.

$$\text{Size} = 485.525 + 2.66075A - 58.26B - 36.9858C + 0.4356\,AB - 0.0956AC + 36.60667BC + 0.011724A^2 - 198.96B^2 + 0.994444C^2 \quad \text{(Eq. 4.1)}$$

Table 4.2. The design of experiments executed for optimization of NLCs dispersion.

S.No.	Lipid (mg)	Surfactant (%)	Sonication (min)	Size (nm)	% Entrapment	PDI
1	125	1.00	3.0	102.40 ± 6.11	40.57 ± 0.57	0.374
2	150	0.50	4.5	169.50 ± 7.59	65.88 ± 0.64	0.312
3	125	0.75	4.5	140.10 ± 13.86	64.17 ± 0.70	0.284
4	100	1.00	4.5	104.48 ± 5.42	49.96 ± 0.87	0.317
5	150	0.75	3.0	187.20 ± 13.89	62.70 ± 0.76	0.284
6	125	0.75	4.5	141.70 ± 12.85	67.20 ± 0.87	0.327
7	125	0.50	6.0	139.39 ± 6.68	40.50 ± 0.80	0.467
8	125	0.50	3.0	201.30 ± 9.93	39.52 ± 0.57	0.240
9	100	0.75	6.0	128.74 ± 8.16	41.53 ± 0.65	0.211
10	125	0.75	4.5	140.20 ± 7.29	68.57 ± 1.24	0.279
11	100	0.75	3.0	162.30 ± 8.65	42.07 ± 0.62	0.357
12	125	0.75	4.5	144.70 ± 15.86	68.10 ± 0.95	0.284
13	125	0.75	4.5	157.40 ± 15.90	65.26 ± 1.26	0.272
14	150	0.75	6.0	139.30 ± 17.86	69.70 ± 1.03	0.211
15	125	1.00	6.0	95.40 ± 10.42	44.22 ± 0.87	0.281
16	150	1.00	4.5	108.87 ± 9.90	68.25 ± 0.77	0.297
17	100	0.50	4.5	176.00 ± 9.47	44.58 ± 0.91	0.258

*The data mentioned is the average of experiments performed in replicates (n=3). PDI was not considered as the response variable. (Low lipid – 100 mg; Medium lipid – 125 mg; High lipid – 150 mg; Low surfactant – 0.50 %; Medium surfactant – 0.75 %; High surfactant – 1.00 %; Low sonication time – 3.00 min; Medium sonication time – 3.50 min; High sonication time – 6.00 %)

The regression equation's (+) positive symbol represents the positive quantitative effect on response value with the respective input variable. The regression equation's (-) negative symbol represents a decrease in response value with the respective input variable. The term A, B, C represents the lipid concentration, surfactant concentration and sonication time respectively. The Quadratic model, with an F-value of 26.00, indicated the significance of the

model. The Lack of Fit was found to be insignificant with a F-value 1.33 relative to the pure error. The insignificant lack of fit in experimental results indicated the best fit for the model. The Adjusted R-square values (0.933604) and Predicted R-square (0.745459) values were found to be in close agreement with each other (difference was less than 0.2). The contour plot and 3D plot obtained for particle size are illustrated in **Figure 4.1 A** and **Figure 4.1 B**. An increase in the particle size with an increase in amount of lipid was observed. The reduction in particle size was observed with an increase in the % surfactant concentration and sonication time. The surfactant reduces the surface tension at the lipid-water interface and enhance the particle's stabilization, reducing the particle size. The increase in sonication minimizes the size of the NLCs, breaking the larger particles into small particles. Adequate precision measures the S/N ratio of the model, which was found to be 17.856 that showed the adequacy of the obtained model.

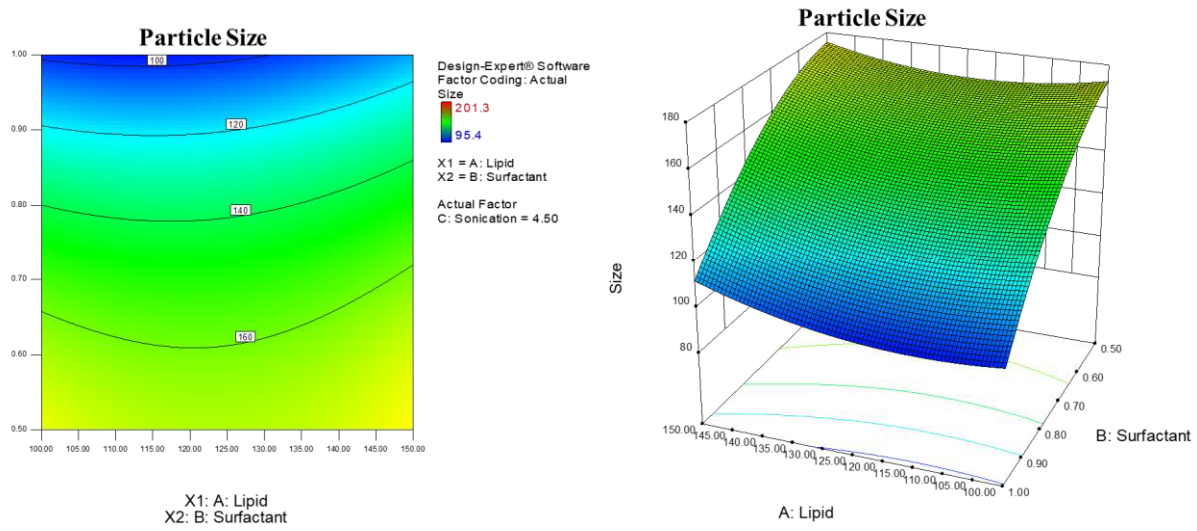

Figure 4.1 A. Box-Behnken optimization contour plot graph showing the effect of independent variables on particle size. **Figure 4.1 B**. Box-Behnken optimization 3D graph showing the effect of independent variables on particle size.

4.3.3.2. Effect of independent variables on entrapment efficiency

The average entrapment efficiency of NLCs dispersion were in the range of 39.52 to 69.70%, as represented in **Table 4.2.** The ANOVA for the responses are demonstrated in **Table 4.3**. The Quadratic model with a 73.63 F-value indicated the significance of the model. The contour plot and 3D graph of the response variable entrapment efficiency are illustrated in **Figure 4.1 C** and **Figure 4.1 D**. The Lack of Fit was insignificant, with a 1.14 F-value relative to the pure error. The coded values of selected independent variables are illustrated as regression equation 4.2.

$$\text{Entrapment efficiency} = -162.248 + 0.35495A + 280.78B + 50.55583C - 0.1204AB + 0.050267AC + 1.78BC + 0.002644A^2 - 178.32B^2 - 6.36111C^2 \quad \text{(Eq. 4.2)}$$

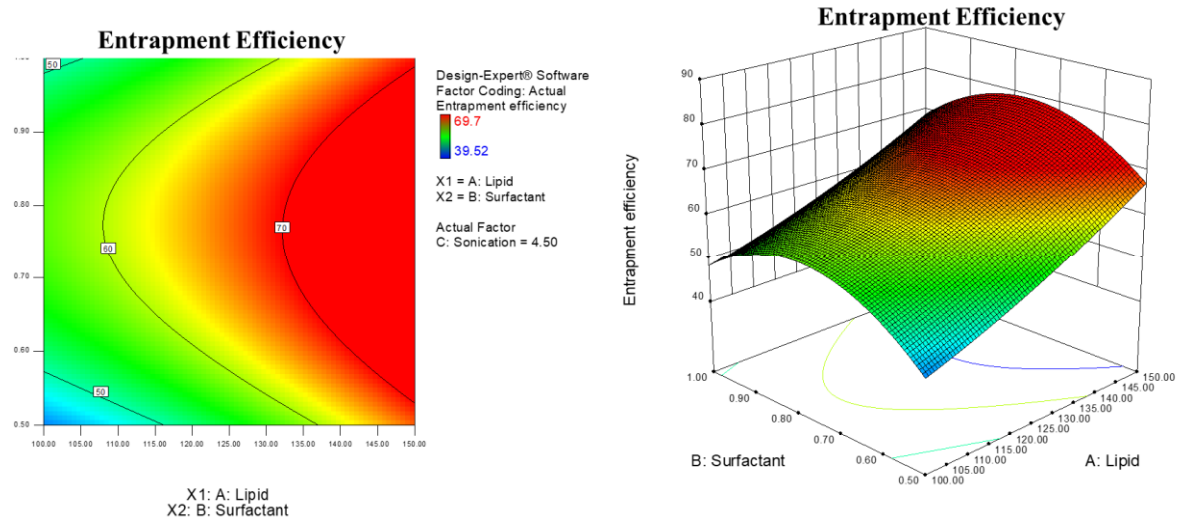

Figure 4.1 C. Box-Behnken optimization contour plot graph showing the effect of independent variables on entrapment efficiency. **Figure 4.1 D.** Box-Behnken optimization 3D graph showing the effect of independent variables on entrapment efficiency.

The adjusted R-square values (0.976109) and predicted R-square (0.91407) values were found to be in close agreement with each other (difference was less than 0.1). The regression equation 4.2 represents the increase in the entrapment with an increase in the amount of lipid. The increase in the entrapment efficiency was observed with an increase in the % surfactant

concentration to some extent. Further increase in the surfactant concentration reduced the entrapment efficiency. The surfactant enhances the particle's stabilization and encapsulation of the drug into nanocarriers. The enhancement in entrapment efficiency was observed with an increase in sonication time. The increase in entrapment was due to the conversion of maximum lipid to nano size particles. When sonication time is less, excess lipid remains as microparticulate particles which are separated from the formulation, thus resulting in low entrapment efficiency. The increase in sonication reduces the size of the NLCs, breaking the larger particles into small particles. Adequate precision measures the S/N ratio of the model, which was found to be 20.252 that showed the adequacy of the obtained model.

Table 4.3. ANOVA for response Particle Size and Entrapment efficiency.

Response	**Particle Size**		**Entrapment efficiency**	
Source	F-value	p-value	F-value	p-value
Model (significant)	73.63278	< 0.0001	25.99771	0.0001
A-Amount of lipid	259.8811	< 0.0001	2.305207	0.1727
B-Surfactant concentration	5.214074	0.0564	156.787	< 0.0001
C-Sonication time	4.09102	0.0828	46.86414	0.0002
AB	0.602742	0.4630	0.491591	0.5059
AC	3.782171	0.0929	0.852406	0.3866
BC	0.474265	0.5132	12.49831	0.0095
A^2	3.059693	0.1237	3.748489	0.0941
B^2	139.173	< 0.0001	10.79534	0.0134
C^2	229.5228	< 0.0001	0.349519	0.5730

4.3.4. Validation of the design to select optimized batch

The optimized NLCs formulation screened by employing numerical and desirability methods. The constraints were selected to achieve high entrapment efficiency and small particle size, as summarized in **Table 4.4.** Based on the 43 solutions illustrated by the Design-Expert software, the batch with high desirability near to 1 was selected. The results were validated using a

formulation with lipid 150 mg, surfactant concentration 0.55%, and sonication time 5 min with the desirability of 0.8069. On execution of the selected formulation, the particle size was found to be 157.91 ± 1.267 nm with 0.165 ± 0.017 PDI. The entrapment efficiency and zeta potential of the formulation were 69.144 ± 0.278% and -16.75 ± 1.40 mV, respectively. This formulation was selected for further characterization. The % deviation of the selected formulation for entrapment efficiency was 0.555 %, and particle size was 6.409 %. This demonstrated that the predicted value was close to the actual value indicating the design's desirability. The desirability graphs of particle size and entrapment efficiency of the validated batch are illustrated in **Figure 4.2**.

Table 4.4. Constraint criteria for achievement of desired response variable and deviation (%) validation batch of NLCs dispersion.

Parameter	**Goal**	**Lower Limit**	**Upper Limit**
A: Amount of lipid (mg)	In range	100	150
B: Surfactant concentration (%)	In range	0.5	1.0
C: Sonication time (min)	In range	3	6
Particle size (nm)	Minimize	95.4	201.3
% EE	Maximize	39.52	69.70
Deviation (%) calculation of Apremilast - NLCs formulation.			
Parameter	**Predicted values**	**Actual values**	**Deviation (%)**
Particle size (nm)	150.789	157.910 ± 1.267	6.409
% EE	69.699	69.144 ± 0.278	0.555

4.3.5. Scale-up studies of the optimized batch

The NLCs dispersion scale-up was performed up to 100 mL, and the formulation was prepared in three different batch sizes (10 mL, 50 mL, and 100 mL) with the parameters obtained in the design space. The composition was similar to the validation batch as mentioned above. The composition (formulation parameters) was kept constant, whereas sonication time was altered as it was a critical criterion in size reduction. The instrument efficiency directly impacted the

size reduction, as the formulation parameters, lipid amount, and surfactant concentration were increased proportionally to batch size. The vessel diameters had a critical role in the size reduction on sonication. The diameters were increased proportionally. The capacity of the probe sonicator was found to have minimum effect. In contrast, the larger diameter vessel altered the formulation parameters to a large extent. There was a need for an increase in sonication time for 100 mL batch size within the design space. The sonication time for 10 mL and 50 mL was 5.0 min, and the sonication time for the 100 mL batch was 6.0 min.

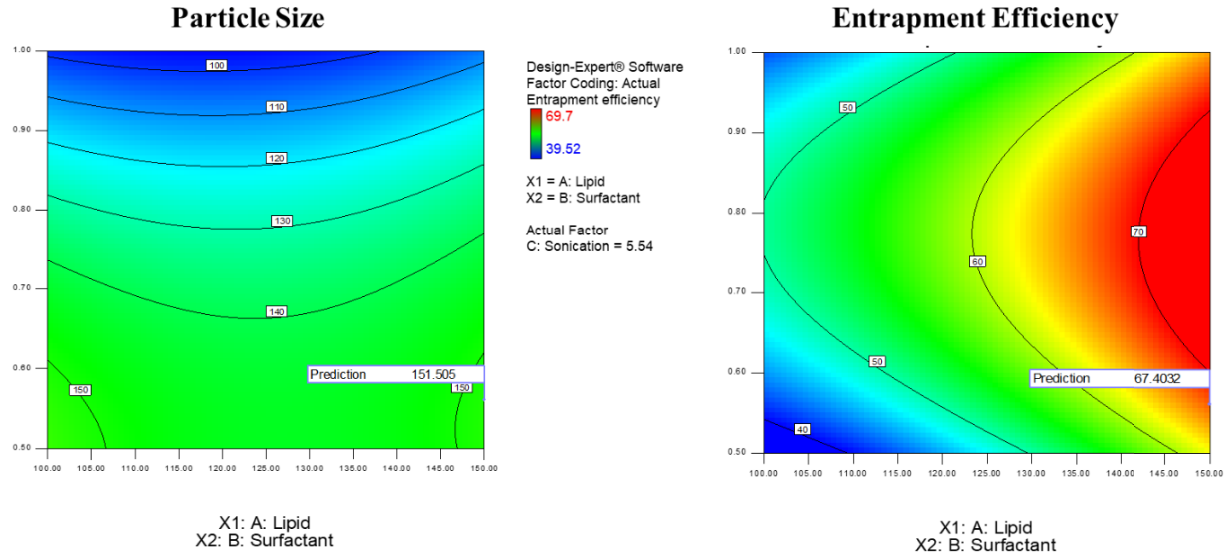

Figure 4.2. The desirability contour plot for particle size and entrapment efficiency.

4.3.6. Characterization of NLCs

4.3.6.1. Attenuated total reflection-Fourier transform infrared spectroscopy (ATR-FTIR)

The FTIR of NLCs dispersion, physical mixture and pure drug were studied to identify any significant change in characteristic peaks due to the interaction between drug and excipients. The FTIR spectra of Apremilast, physical mixture, and Apremilast loaded NLCs are presented in **Figure 4.3.** The Apremilast characteristic peaks include the range of 3100 and 3500 cm^{-1} indicating the amide group of Apremilast. The C=C (alkene) and C-C (alkane) peaks range

from 1600 cm^{-1} and 1300 cm^{-1}. The peaks in the range of 1100 cm^{-1} and 1000 cm^{-1} indicate the C-OH and C-O (ester bond), respectively.

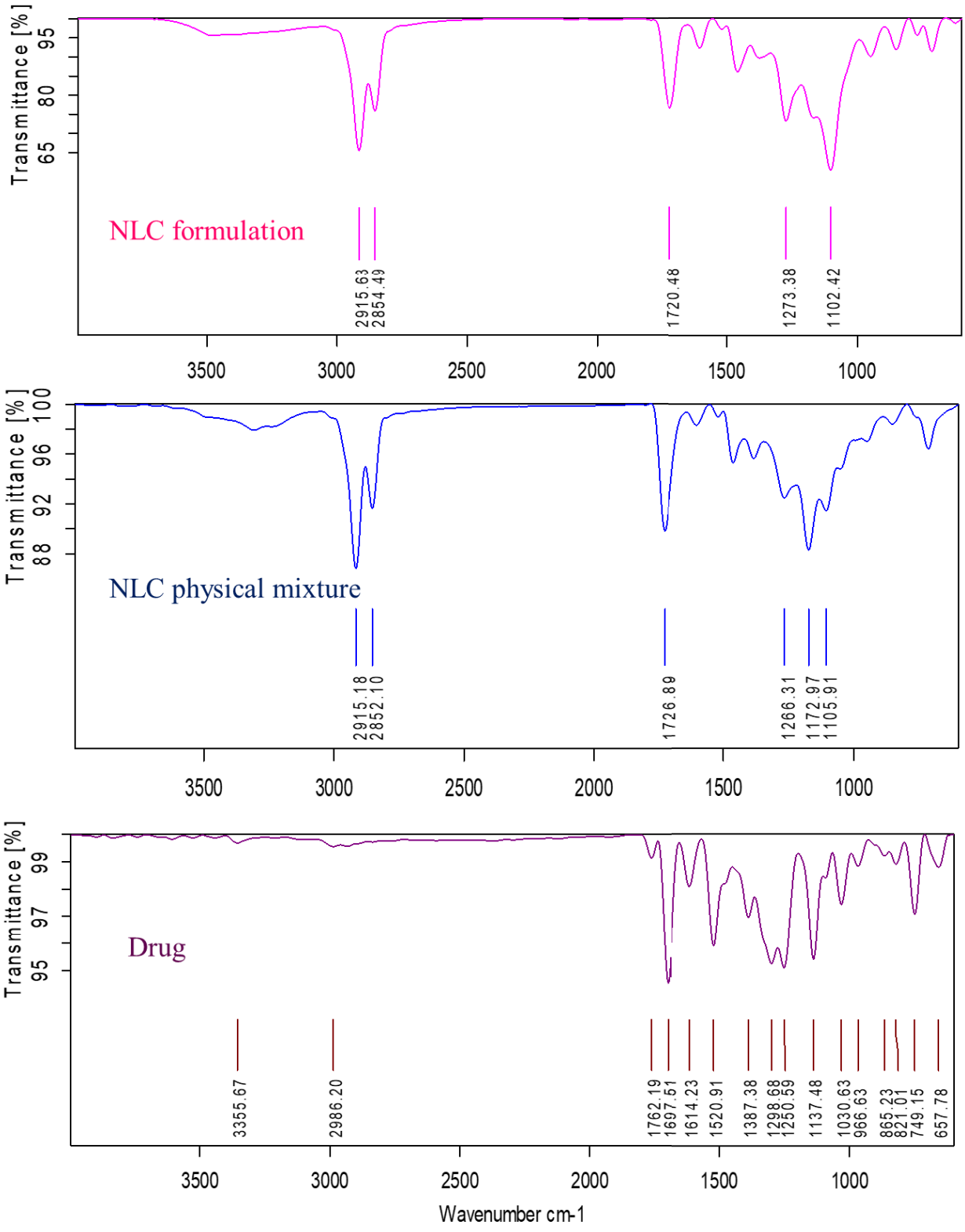

Figure 4.3. The FTIR spectra of Apremilast, physical mixture, and Apremilast loaded NLCs.

The spectra revealed the absence of physicochemical interactions between the drug and other formulation excipients. The study indicated no chemical interaction and good compatibility of the excipients with Apremilast in the NLCs formulation.

4.3.6.2. Particle size, zeta potential measurement and entrapment efficiency

The particle size of the executed formulations with 10 mL, 50 mL and 100 mL batch size were 157.50 ± 2.007 nm (0.158 PDI), 142.57 ± 2.815 nm (0.195 PDI) and 158.53 ± 1.041 nm (0.208 PDI), respectively (shown in **Figure 4.4**). The optimized formulation exhibited a zeta potential of -17.7 ± 0.47 mV (shown in **Figure 4.5)**. The zeta potential above ± 10 indicates stable electrostatic repulsion of the prepared dispersion, which minimizes the particles' coalescence/aggregation. Entrapment efficiency of 10 mL, 50 mL and 100 mL batches were 69.36 ± 0.59%, 70.55 ± 0.78%, 68.09 ± 0.49%, respectively. The morphology of NLCs dispersion is portrayed in **Figure 4.6.** The results indicated that the particles were spherical in shape with particle size in the range of 100 nm to 140 nm. The particle size less than 200 nm with PDI less than 0.300 is suitable for topical application to improve the permeation [8,9].

4.3.6.3. In-vitro drug release studies

The results of the NLCs dispersion in-vitro release study are illustrated in **Figure 4.7.** The free drug showed 100% release in 6 h. The NLCs dispersion (10 mL, 50 mL, and 100 mL batch size) showed drug release up to 24 h. The interpretation of drug release using mathematical models represents that the NLCs dispersion followed the first-order model as the best fit with the highest r^2 value and minimum Akaike information criterion. The n value obtained was less than 0.45 indicating Fickian type diffusion. The values obtained were described in **Table 4.5.** The controlled release pattern was expected due to the drug dissolved in the lipid matrix. The slow drug release from NLCs dispersion is expected to provide prolonged action in the skin layers.

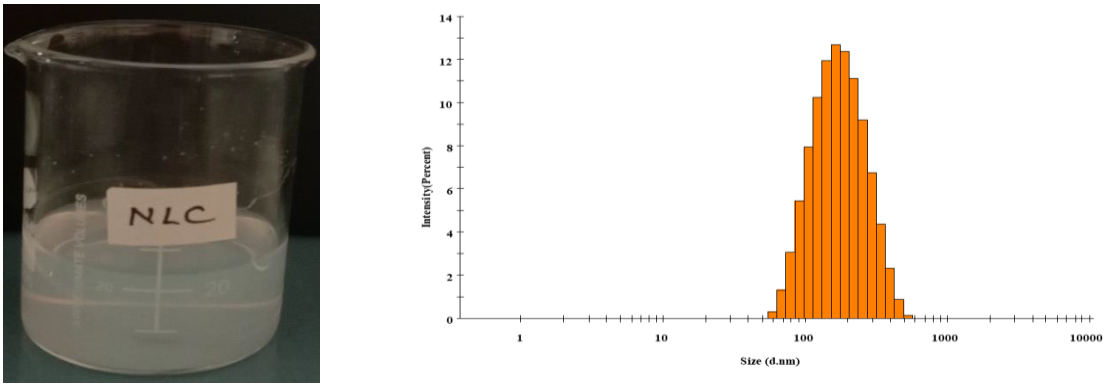

Figure 4.4. Apremilast loaded NLCs dispersion and particle size statistics graph.

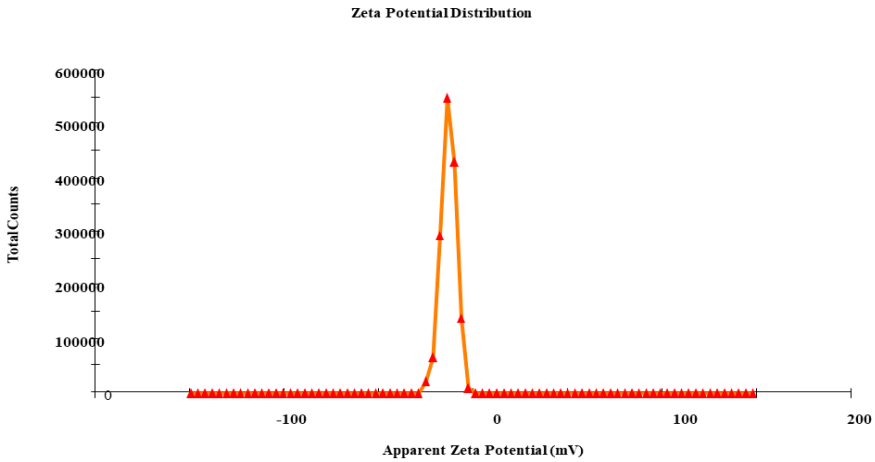

Figure 4.5. Apremilast loaded NLCs dispersion zeta potential graph.

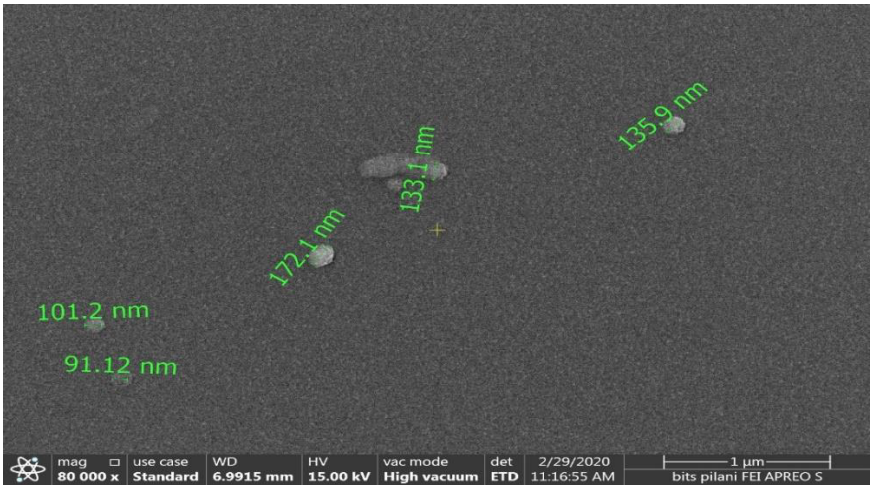

Figure 4.6. Morphology of Apremilast loaded NLCs dispersion performed using Field Emission Scanning Electron Microscopy.

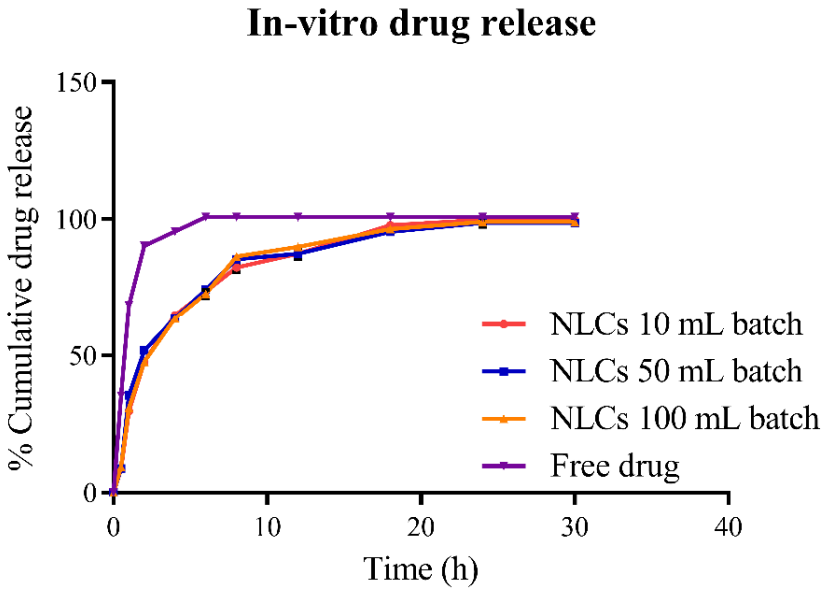

Figure 4.7. The in-vitro drug release profile of Apremilast loaded NLCs dispersion (10 mL, 50 mL and 100 mL) and free drug.

Table 4.5. Release kinetic mechanism data of Apremilast loaded NLCs dispersion.

Batch Size		Zero-order	First-order	Higuchi	Korsmeyer-Peppas	Hixson-Crowell
10 mL	R^2	0.146	0.983	0.834	0.926 (n=0.327)	0.909
10 mL	AIC	104.700	61.760	86.666	78.582	80.041
50 mL	R^2	0.026	0.969	0.791	0.927 (n=0.305)	0.869
50 mL	AIC	105.590	67.779	88.651	79.035	83.557
100 mL	R^2	0.104	0.985	0.818	0.928 (n=0.319)	0.905
100 mL	AIC	105.148	60.499	87.599	79.332	80.455

4.3.6.4. Cytotoxicity study

The selected NLCs dispersion formulation was evaluated for cytotoxicity study on HaCaT cell lines (immortalized human keratinocyte). The 95% of epidermal skin cells were keratinocytes. Hence these cells were preferred for this study. The results showed the formulation excipients were non-toxic against HaCaT cells in comparison to the free Apremilast solution. The results are summarized in **Figure 4.8** more than 50% of cell viability was noted with 20 nm concentration with Apremilast loaded NLCs dispersion and free Apremilast solution [10].

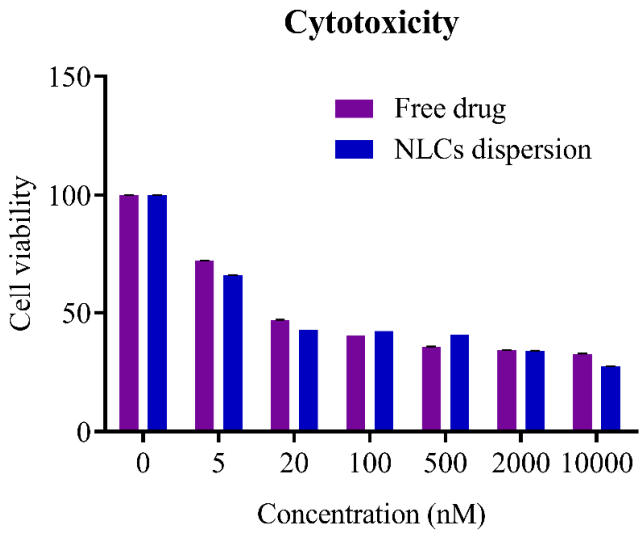

Figure 4.8. Graphic representation of cell viability of Apremilast loaded NLCs dispersion and free drug.

4.3.6.5. Cell uptake

The Coumarin-6 loaded NLCs uptake was performed for 1 h, and 3 h in three groups, untreated HaCaT cells, HaCaT cells treated with Coumarin-6 dispersions, and Coumarin-6 loaded NLCs. The Coumarin-6/DAPI ratio of NLCs dispersion was found to be higher at 1 h and 3 h intervals. The uptake of Coumarin-6 loaded NLCs dispersion was 9.39 and 41.86 fold higher in 1 h and 3 h, respectively, compared to Coumarin-6 dispersion. The fluorescence microscope images of cell uptake data and cell uptake intensity are illustrated in **Figures 4.9 A and 4.9 B.** The enhanced uptake can be attributed to the interaction between the cell membrane, the fatty acid chain of the lipid, and the nano size of the NLCs [11].

4.3.6.6. Expression of TNF-α in psoriasis induced model

The NLCs dispersion and free Apremilast were evaluated for the reduction in TNF-α in-vitro imiquimod-induced psoriasis. Initially, RNA was isolated, and gene expression was quantified and normalized to GAPDH. After treating NLCs and free Apremilast, there was a discernible change in cycle threshold (Ct) values. There was a 6.4 fold and 1.6 fold more significant C_t value reduction with NLCs dispersion and the free drug compared to the positive control. The

results are exemplified in **Figure 4.10**. The Apremilast reduces cAMP degradation, which further reduces the relative mRNA expression of TNF-α. The high internalization ability of Apremilast by NLCs dispersion favors improved efficacy in comparison to free Apremilast. The increase in cell internalization reduces the inflammatory mediators TNF-α [12–14].

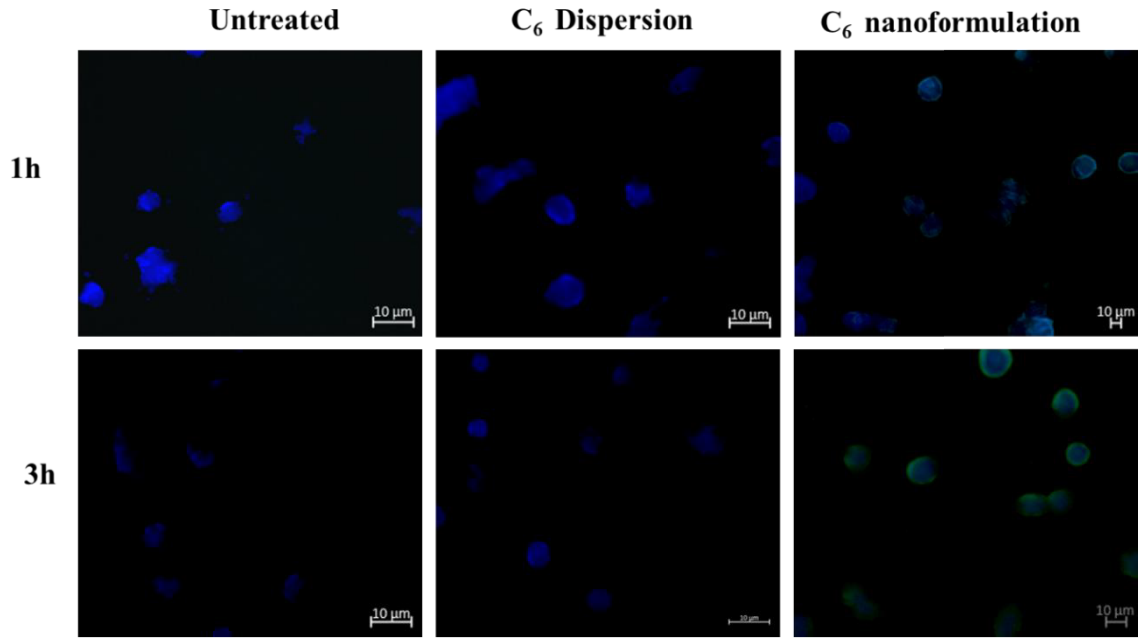

Figure 4.9 A. The cell uptake Fluorescence microscopic images.

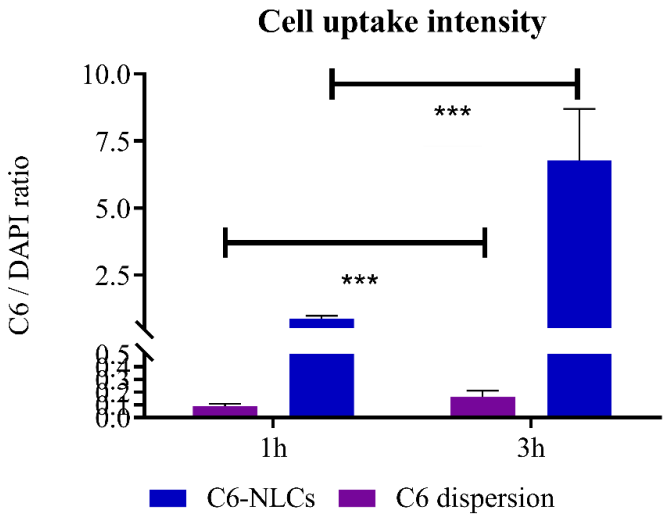

Figure 4.9 B. Cell uptake intensity of Coumarin-6 loaded NLCs and free Coumarin-6 (***p<0.0001).

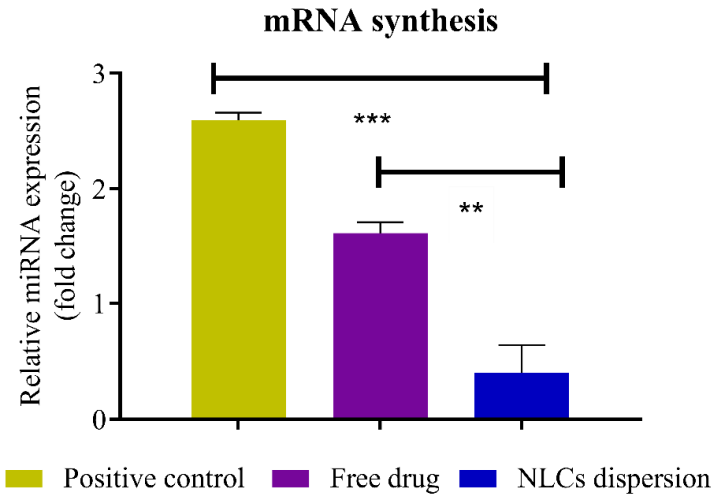

Figure 4.10. The relative reduction of TNF-α mRNA in the imiquimod induced psoriasis model (n=3) (**p<0.005).

4.3.7. Characterization of Apremilast loaded NLCs gel

4.3.7.1. Rheological behavior

The Apremilast loaded NLCs gel formulation was evaluated with cone type (CP25) configuration with a 0.05 mm gap. The viscosity of the prepared 0.75% gel was found to be 6044 mPa.s at a constant shear rate, as illustrated in **Figure 4.11 A.** Due to the constant shear rate, Carbopol gel remains fully structured. There was no change found in Carbopol gel viscosity, which was expected due to its Newtonian behavior at lower concentrations [15,16]. The Apremilast loaded NLCs gel exhibited linear viscoelastic properties and solid-like properties at low strain with amplitude sweep test. The storage modulus of the gel was depleted outside the critical strain of 0.061%. The result indicated that the gel could hold back maximum strain before structural deformation (**Figure 4.11 B)**. The frequency sweep test showed high stability of gel as the results revealed no change in storage modulus (G'). The results exhibited a high degree of crosslinking, which was expected due to an increase in structural strength (**Figure 4.11 C & 4.11 D)**. The rheological study of Apremilast loaded NLCs gel revealed good structural stability with significantly higher storage modulus (G') compared to loss modulus (G") [17,18].

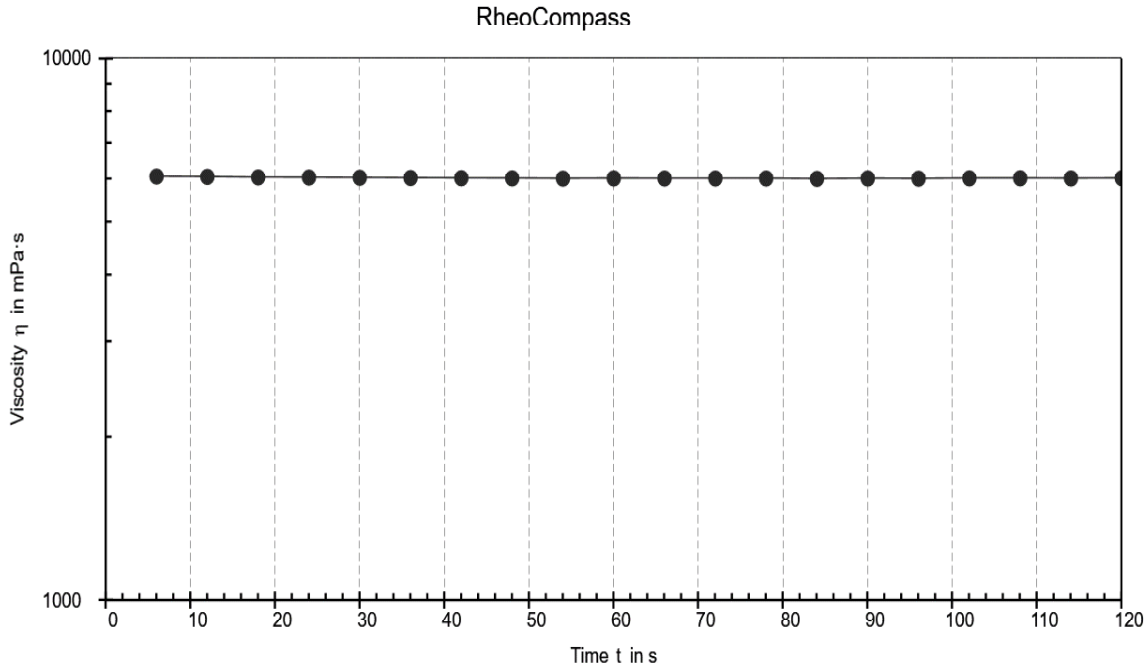

Figure 4.11 A. The viscosity of Apremilast loaded NLCs gel

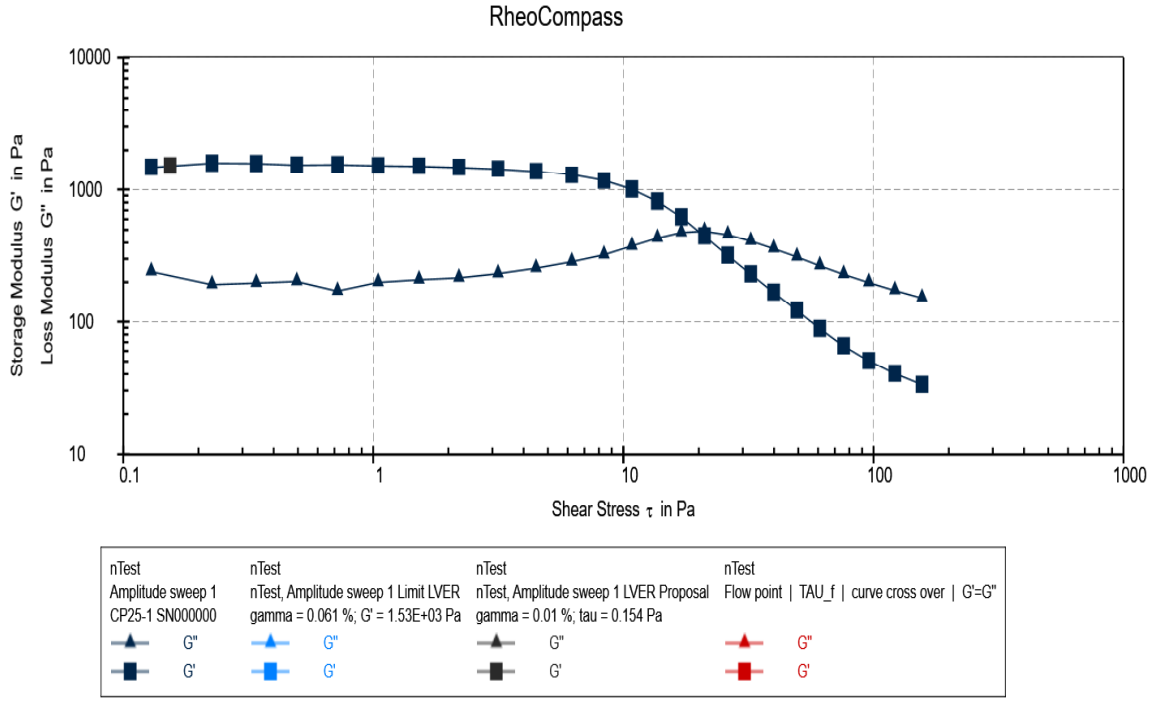

Figure 4.11 B. Amplitude sweep test of Apremilast loaded NLCs gel

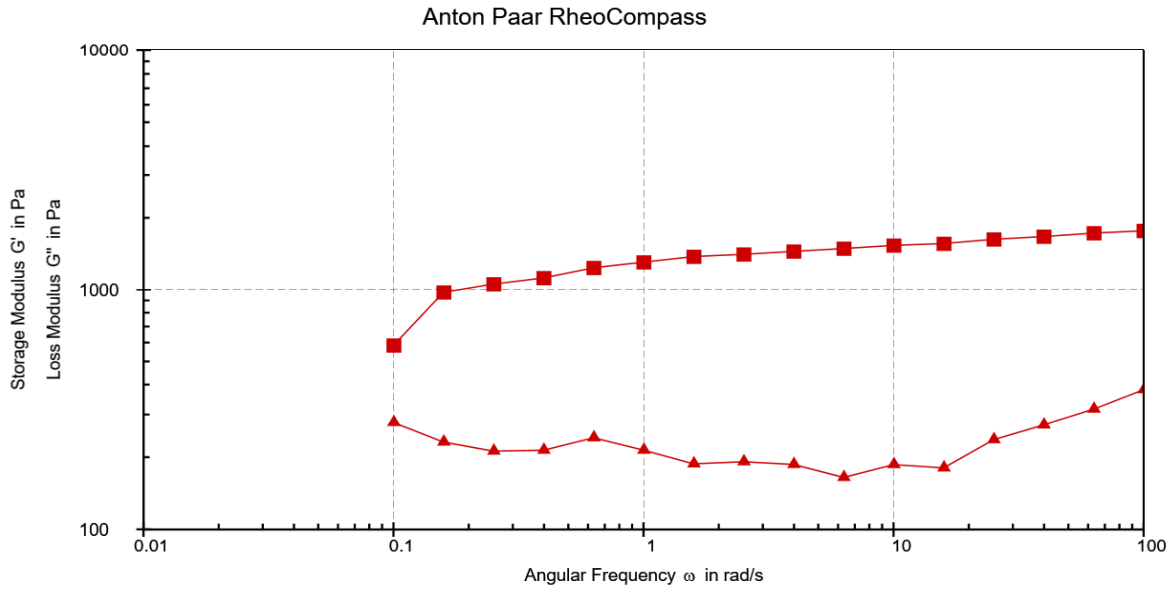

Figure 4.11 C. Frequency sweep test of Apremilast loaded NLCs gel (loss modulus and storage modulus).

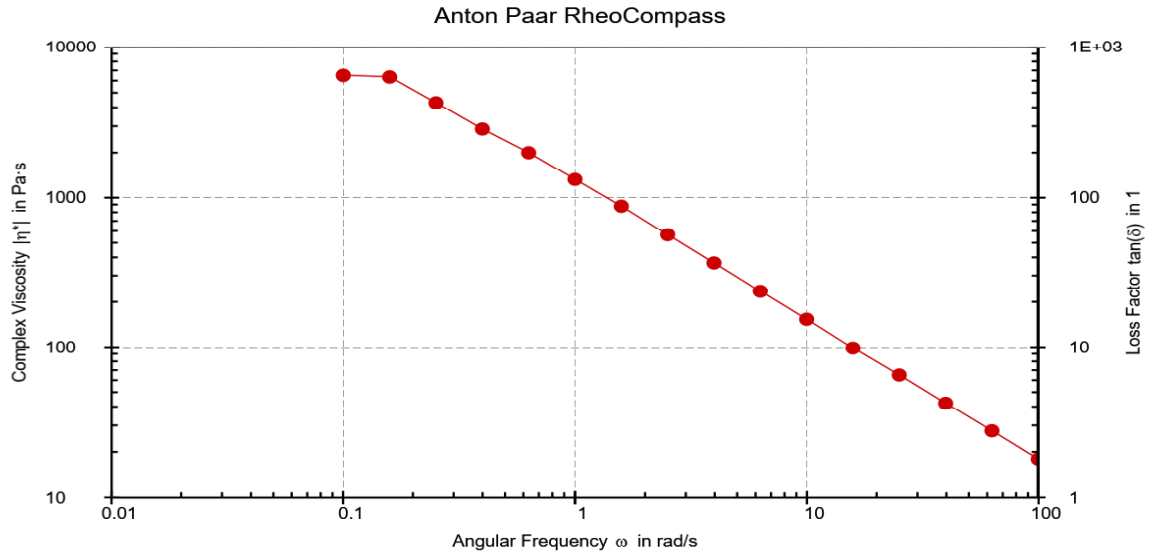

Figure 4.11 D. Frequency sweep test of Apremilast loaded NLCs gel formulation (Complex viscosity).

4.3.7.2. Occlusive Test

The Apremilast loaded NLCs gel formulations were evaluated for occlusive ability in in-vitro conditions. The results of the occlusion test are represented in **Figure 4.12 A**. The results revealed that Apremilast loaded NLCs gel reduced percentage water loss through cellulose acetate membrane compared to free drug-loaded gel. The occlusive factor of NLCs loaded gel

was 54.769 ± 0.282 and free drug-loaded gel was 8.302 ± 0.587 in 48 h. The small size of NLCs loaded gel favors the formation of an occlusive layer after the topical application on the skin and reduces the percentage of TEWL. The high occlusive ability of Apremilast loaded NLCs gel improves skin permeation on the topical application due to decreased TEWL [19].

4.3.7.3. Ex-vivo skin permeation studies

The cumulative amount of drug permeated through the skin for NLCs loaded gel and free drug-loaded gel after 24 h was found to be 8.024 ± 1.397 µg/cm^2 and 3.951 ± 0.627 µg/cm^2, respectively. The transdermal permeation is shown in **Figure 4.12 B.** The transdermal flux of NLCs formulation was 0.315 µg/h/cm^{2,} and free drug formulation was 0.167 µg/h/cm^2, which was found to be 1.88 fold less. The permeability coefficient of NLCs formulation and the free drug-loaded gel was 0.11 ×10^{-2} and 0.06×10^{-2}, respectively. The nanosize of dispersion and formation of an occlusive film on the skin was found to be the reason for improved permeation of the NLCs formulation. Skin hydration leads to swelling of skin lipids and improves skin permeation [9,20].

4.3.7.4. Dermal retention studies

The skin retention of the Apremilast through NLCs formulation was found to be 15.22 ± 0.88 µg/cm^2 and 20.89 ± 1.33 µg/cm^2 in stratum corneum and viable part of the skin. Whereas, in free drug-loaded gel, the drug retained in the stratum corneum and viable part of skin was 8.85 ± 1.14 µg/cm^2 and 3.55 ± 1.06 µg/cm^2, respectively. The study demonstrated improved skin retention and permeation with Apremilast loaded NLCs gel **Figure 4.12 C**. The drug retention with NLCs formulation was 1.72 fold higher in the stratum corneum and 5.90 fold higher in the viable part of skin than free drug-loaded gel. The total skin permeation and retention studies depicted the low transdermal flux and high skin retention in skin layers.

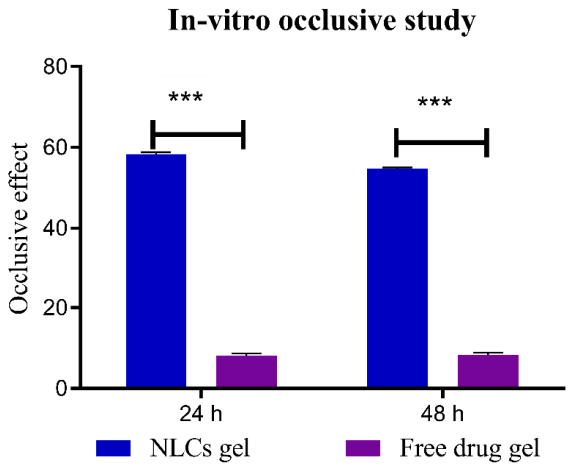

Figure 4.12 A. Occlusive effect of Apremilast loaded NLCs gel and free drug-loaded gel (Mean ± SD, n = 3) (***p<0.0001).

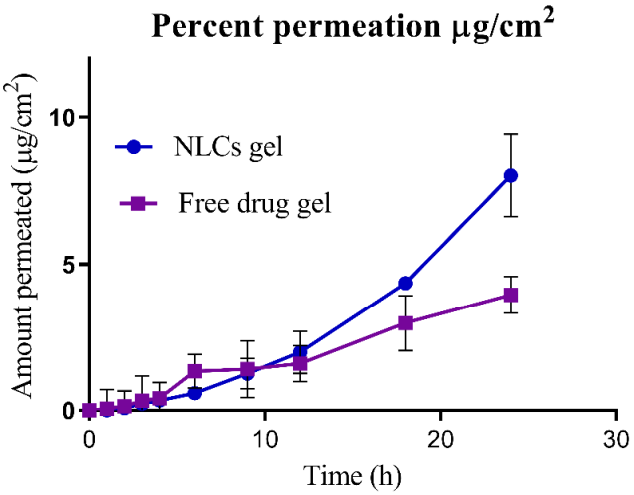

Figure 4.12 B. Ex-vivo skin permeation profiles of Apremilast loaded NLCs gel compared with free drug-loaded gel (Mean ± SD, n=3).

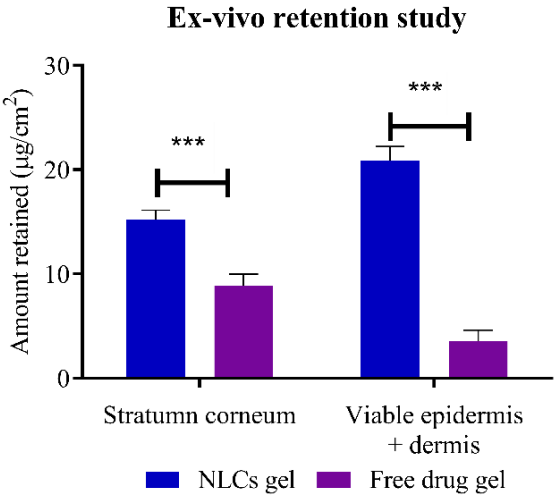

Figure 4.12 C. Skin retention study of Apremilast loaded NLCs gel compared with free drug-loaded gel (Mean ± SD, n=3) (***p<0.0001).

The improved permeation can attribute to the reduced TEWL and the high amount of drug in the viable epidermis was expected due to the liquid lipid used in the NLCs formulation. The increase hydration of the skin ascribed by NLCs loaded hydrogel. The alteration in cellular and physiological environment of skin due to the lipid vehicle and micro-reservoir formation in skin layers improve retention [21]. The results imply the advantage of NLCs in the treatment of chronic skin disorders targeting skin layers with minimal systemic absorption. The drug-loaded in NLCs diffuses through intracellular and follicular routes due to smaller size [8].

4.3.7.5. Ex-vivo dermal distribution studies

The qualitative skin distribution studies of NLCs dispersion were determined using Coumarin-6 loaded NLCs formulation and Coumarin-6 aqueous dispersion. The Coumarin-6 dye was selected for this study due to its low permeability into the skin layers. The results of the study performed for 8 h and 16 h are presented in **Figure 4.13.** The results demonstrated the high permeation of Coumarin-6 dye into deeper skin layers from its NLCs dispersion compared to the free Coumarin-6 dye dispersion. The greater permeation of NLCs preparation was expected due to nanosize, occlusive nature and diffusion through the stratum corneum [22].

4.3.7.6. Dermatokinetic estimation

The dermatokinetic profile of Apremilast loaded NLCs gel formulation and the free drug-loaded gel is shown in **Figure 4.14 A** and **Figure 4.14 B**. The $C_{maxSkin}$ of the Apremilast loaded NLCs gel was found to be 109.123 ± 4.837 µg/cm^2 in the epidermis and 62.444 ± 3.535 µg/cm^2 in the dermis. The $C_{maxSkin}$ of the free drug-loaded gel was found to be 41.768 ± 2.518 µg/cm^2 in the epidermis and 13.047 ± 3.107 µg/cm^2 in the dermis. The T_{max} of the Apremilast loaded NLCs gel was found to be 8 h in the epidermis and dermis, whereas for free drug-loaded gel, it was found to be 6 h in the epidermis and 8 h in the dermis. The $AUC_{0–24}$ of the Apremilast-loaded NLCs gel was 6.50 fold higher in epidermis (2112.538 ± 140.428 µg/cm^2.h) compared

to free drug-loaded gel (324.840 ± 8.828). In dermis the Apremilast-loaded NLCs gel (847.120 ± 83.051 µg/cm^2.h) exhibited 4.14 fold higher compared to free drug-loaded gel (204.343 ± 8.482 µg/cm^2.h). The pharmacokinetic parameters of Apremilast loaded NLCs gel and free drug-loaded gel are summarized in **Table 4.6**. The higher drug concentration in skin layers and higher T_{max} obtained from NLCs based gel demonstrated improved permeation and skin retention compared to conventional gel preparation. The results indicate that NLCs are expected to embed in the superficial layers (epidermis) and followed by diffusion into deeper layers (dermis). The lipid-based gel formulation exhibits adhesive property, which favors a high concentration of the drug in the skin layers [23].

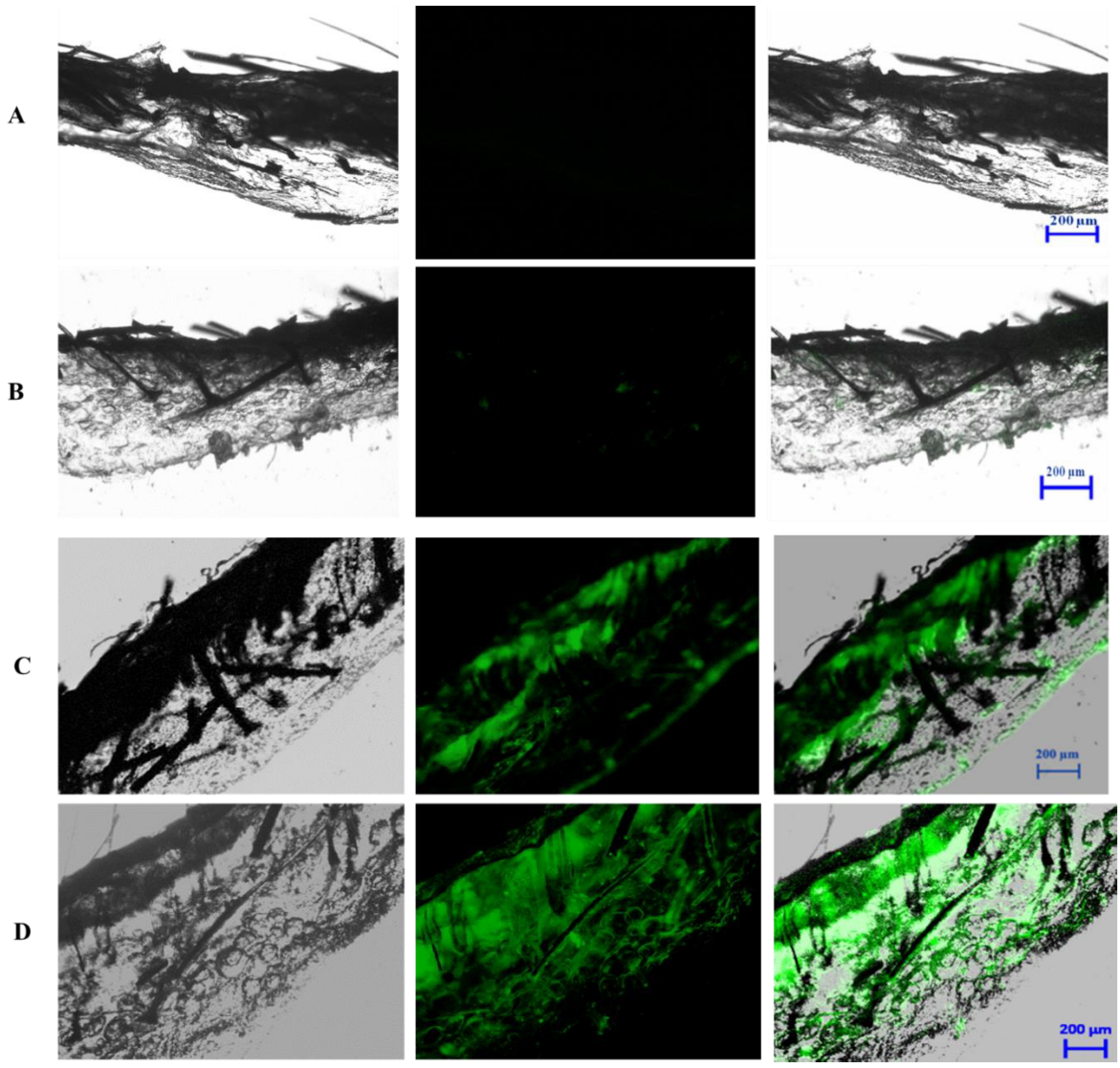

Figure 4.13. In-vitro skin retention studies using Coumarin-6 loaded NLCs and free Coumarin-6. **(A)** Skin treated with free Coumarin-6 for 8h; **(B)** Skin treated with free Coumarin-6 for 16h; **(C)** Skin treated with Coumarin-6 loaded NLCs for 8 h; **(D)** Skin treated with Coumarin-6 loaded NLCs for 16h.

Table 4.6. Summary of dermatopharmacokinetic evaluation of Apremilast loaded NLCs gel and free drug-loaded gel (n=4).

Parameter	Apremilast loaded NLCs gel		Free drug-loaded gel	
	Epidermis	Dermis	Epidermis	Dermis
AUC_{0-24} ($\mu g/cm^2.h$)	2112.538 ± 140.428	847.120 ± 83.051	324.840 ± 8.828	204.343 ± 8.482
AUC_{0-inf} ($\mu g/cm^2.h$)	3869.724 ± 743.023	1337.911 ± 119.986	465.389 ± 7.100	442.657 ± 62.786
$C_{maxSkin}$ ($\mu g/cm^2$)	109.123 ± 4.838	62.444 ± 3.563	41.768 ± 2.518	13.047 ± 3.107
T_{max} (h)	8.000	8.000	6.000	8.000
Ke (h^{-1})	0.034 ± 0.014	0.050 ± 0.001	0.052 ± 0.001	0.030 ± 0.010

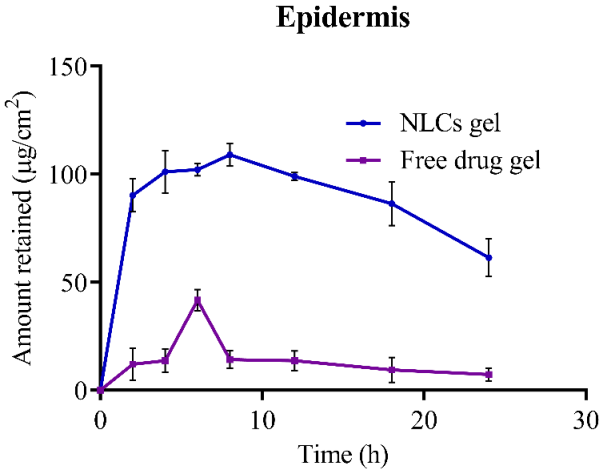

Figure 4.14 A. Dermatokinetic profile of Apremilast loaded NLCs gel compared with free drug-loaded gel in the epidermis (Mean ± SD, n=4) (***p<0.0001)

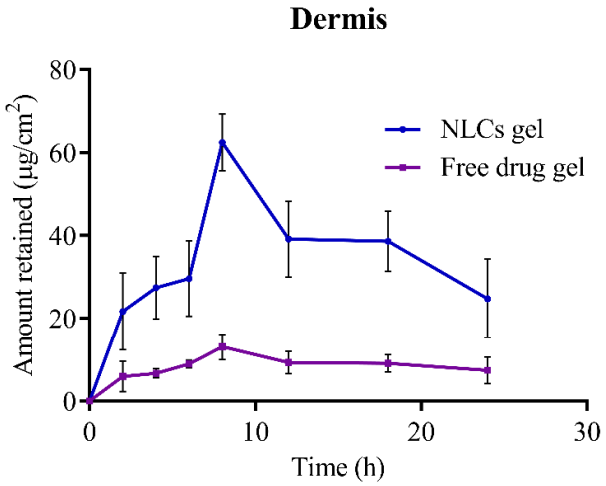

Figure 4.14 B. Dermatokinetic profile of Apremilast loaded NLCs gel compared with free drug-loaded gel in the dermis (Mean ± SD, n=4) (***p<0.0001).

4.3.8. In-vivo skin retention and irritation studies

The amount of drug retained (µg/cm^2) in skin layers of swiss albino mice treated with Apremilast loaded NLCs gel and free drug-loaded gel after 12 h and 24 h are illustrated in **Figure 4.15**. The amount of drug retained in the skin was higher in NLCs loaded gel formulation (3.78 fold in 12 h, 3.22 fold higher in 24 h) than free drug-loaded gel. The drug retained in the stratum corneum and viable part of the skin treated with Apremilast loaded NLCs gel, and free drug-loaded gel are represented in **Table 4.7.**

Table 4.7. Amount of Apremilast retained in the skin layers

Formulation		**Skin layers**	
		Stratum Corneum (µg/cm^2)	**Viable epidermis + dermis (µg/cm^2)**
NLCs gel	**12 h**	11.15 ± 1.13	4.81 ± 1.78
	24 h	7.02 ± 0.68	4.16 ± 2.26
Free drug loaded gel	**12 h**	2.16 ± 0.60	2.06 ± 0.56
	24 h	1.62 ± 0.85	1.85 ± 0.82

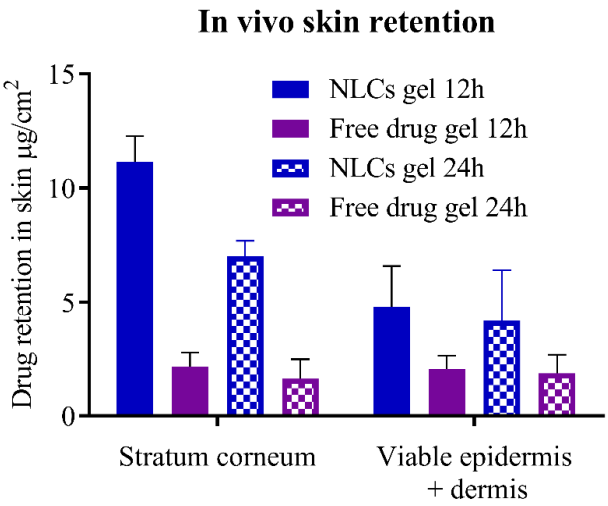

Figure 4.15. Skin retention of Apremilast in swiss albino mice treated with NLCs loaded gel and free drug-loaded gel for 12 h and 24 h.

The data revealed a high drug concentration in 12 h compared to 24 h in animals treated with Apremilast-loaded NLCs gel. As the data obtained in the dermatokinetic study, T_{max} achieved was 8 h, indicating a higher drug concentration in 12h compared to 24 h. The amount of drug retained was higher in Apremilast loaded NLCs gel compared to free drug preparation. The amount of drug in the stratum corneum after 12 h was similar in three formulations. The NLCs gel exhibited increased permeation compared to SLNs, which was expected due to the Labrafac M 2125 (medium-chain triglycerides), which favors the improved permeation in deeper layers. The drug retained in skin layers up to 24 h indicates that the developed NLCs formulation can exhibit prolonged retention in skin layers [24,25].

The skin irritation studies showed no signs of irritation (inflammation and erythema) on the skin in 12h and 24h after applying the gel, as illustrated in **Figure 4.16**. The skin histology study showed that there were no signs of inflammation or changes in the skin. The H&E staining histology data is represented in **Figure 4.17**. The data showed the skin structure was intact and normal [26,27]. The results indicate the developed NLCs formulation is safe for topical delivery of Apremilast. The developed NLCs formulation can improve permeation and skin retention for a prolonged time duration.

4.3.9. Storage stability of Apremilast loaded NLCs gel

The Apremilast loaded NLCs gel redispersed in water exhibited no aggregation. The assay results depicted no significant change (< 2%), represented in **Table 4.8,** indicating the stability of Apremilast loaded NLCs gel [28,29].

Table 4.8. Stability data of Apremilast loaded NLCs gel (n=3).

Stability data of NLCs dispersion loaded gel at 4˚C				
Parameter	**0 Month**	**1 Month**	**2 Month**	**3 Month**
Assay of gel (%)	100.00 ± 0.817	99.97 ± 0.380	99.94 ± 0.688	99.91 ± 0.829
Size (nm)	162.83 ± 3.160	164.24 ± 3.060	173.72 ± 4.323	177.00 ± 2.857
PDI	0.232 ± 0.018	0.244 ± 0.004	0.249 ± 0.09	0.237 ± 0.002
Stability data of NLCs dispersion loaded gel at 25 ˚C				
Assay of gel (%)	100.00 ± 0.817	99.83 ± 0.761	99.64 ± 0.604	99.12 ± 0.396
Size (nm)	162.83 ± 3.160	163.78 ± 3.293	179.10 ± 2.708	183.44 ± 4.973
PDI	0.232 ± 0.018	0.218 ± 0.011	0.297 ± 0.061	0.263 ± 0.009

Formulation	Before application of gel	After application of gel
NLCs loaded gel	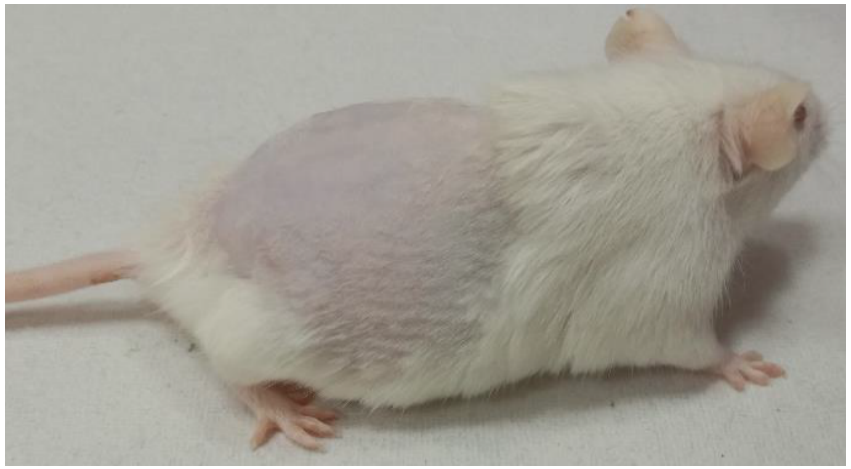	
Free drug-loaded gel	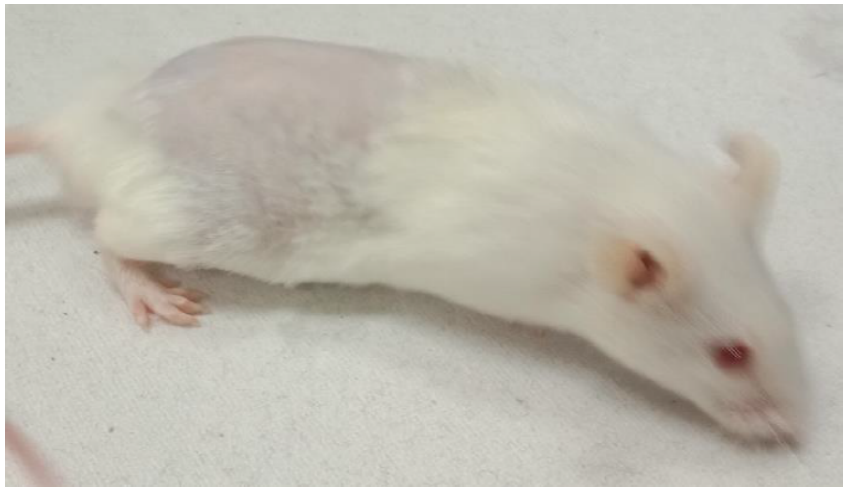	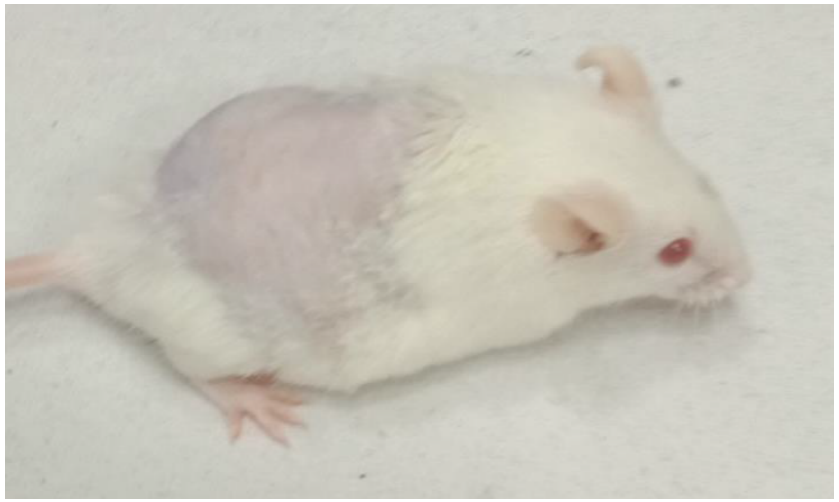

Figure 4.16 The animal images for signs of irritation (inflammation and erythema) after and before application.

Formulation	12 h	24 h
NLCs loaded gel	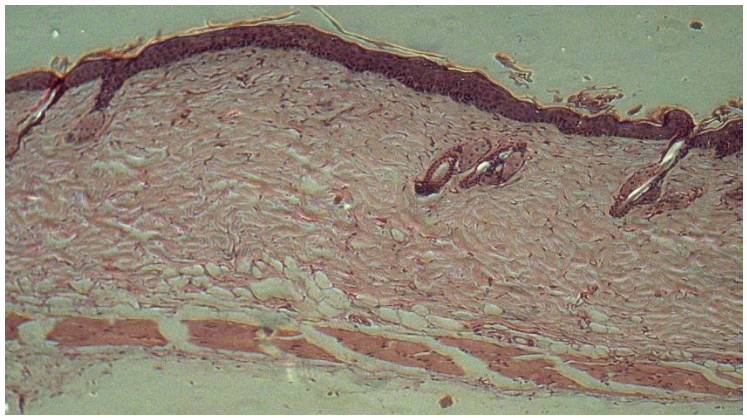	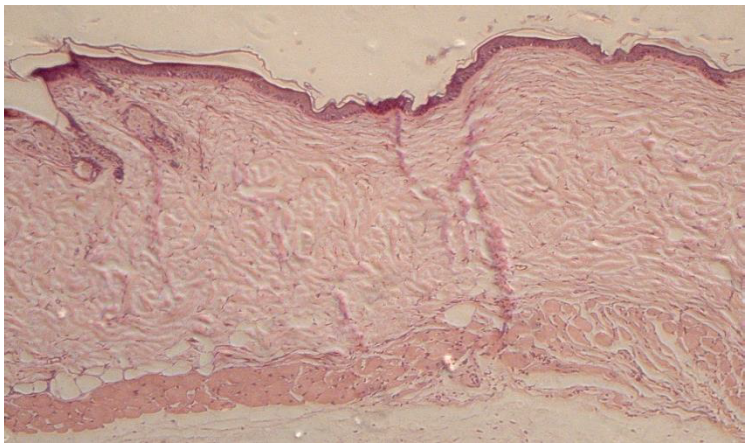
Free drug-loaded gel	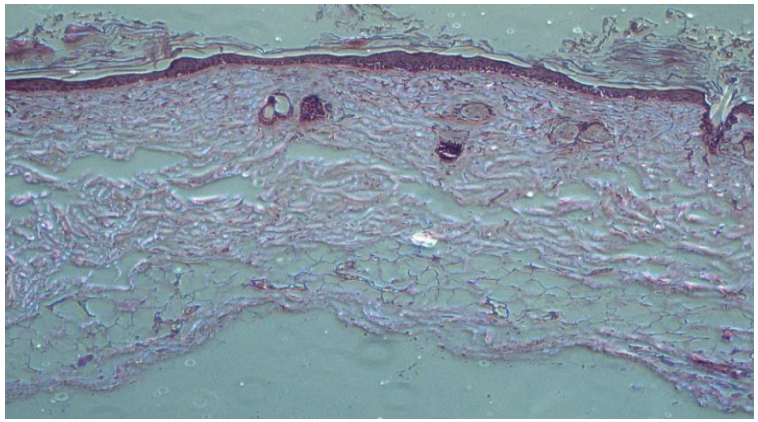	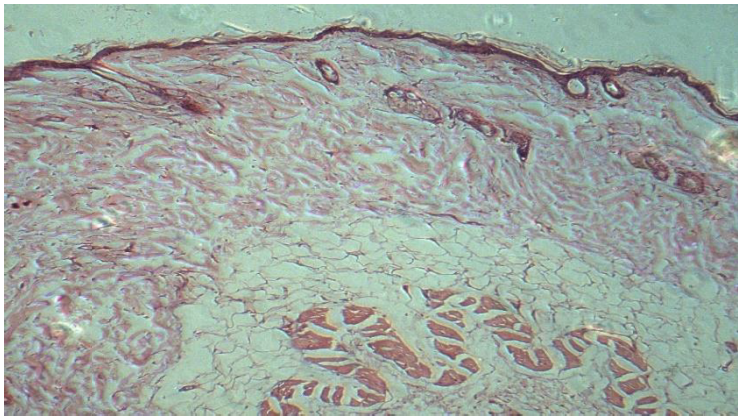

Control (without application of formulation)

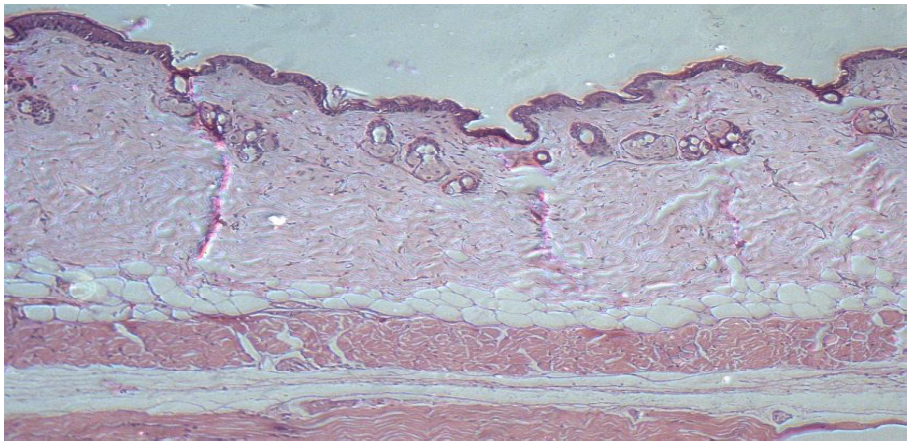

Figure 4.17. The H&E staining histology data after 12 h and 24 h of application

4.4. Conclusion

NLCs loaded Apremilast was formulated by hot emulsification technique and optimized using Box Behnken design. The optimized formulation exhibits small particle size and PDI to improve permeation into the skin. The small particle size was affected by surfactant, and the lower HLB value of lipid increases entrapment efficiency. The optimized formulation exhibited control release for 24 h. The NLCs loaded gel has improved permeation and skin retention. The increase in the anti-psoriasis activity was observed in the in-vitro psoriasis efficacy study. In-vitro cytotoxicity and in-vivo skin irritation study revealed the optimized formulation was non-toxic, and no irritation/erythema was observed. The obtained results showed the NLCs loaded Apremilast could be explored for topical delivery with enhanced skin retention and psoriasis efficacy.

References

[1] V.K. Rapalli, G. Singhvi, S. Gorantla, T. Waghule, S.K. Dubey, R.N. Saha, M.S. Hasnain, A.K. Nayak, Stability indicating liquid chromatographic method for simultaneous quantification of betamethasone valerate and tazarotene in in vitro and ex vivo studies of complex nanoformulation, J. Sep. Sci. 42 (2019) 3413–3420. https://doi.org/10.1002/jssc.201900538.

[2] J.R. Madan, S. Khobaragade, K. Dua, R. Awasthi, Formulation, optimization, and in vitro evaluation of nanostructured lipid carriers for topical delivery of Apremilast, Dermatol. Ther. 33 (2020). https://doi.org/10.1111/dth.13370.

[3] P.K. Parmar, A.K. Bansal, Novel nanocrystal-based formulations of apremilast for improved topical delivery, Drug Deliv. Transl. Res. (2020) 1–18. https://doi.org/10.1007/s13346-020-00809-1.

[4] V.K. Rapalli, T. Waghule, S. Gorantla, S.K. Dubey, R.N. Saha, G. Singhvi, Psoriasis: pathological mechanisms, current pharmacological therapies, and emerging drug delivery systems, Drug Discov. Today. (2020). https://doi.org/10.1016/j.drudis.2020.09.023.

[5] V.K. Rapalli, V. Kaul, T. Waghule, S. Gorantla, S. Sharma, A. Roy, S.K. Dubey, G. Singhvi, Curcumin loaded nanostructured lipid carriers for enhanced skin retained topical delivery: optimization, scale-up, in-vitro characterization and assessment of ex-vivo skin deposition, Eur. J. Pharm. Sci. 152 (2020) 105438. https://doi.org/10.1016/j.ejps.2020.105438.

[6] S. Jain, S. Krishna Cherukupalli, A. Mahmood, S. Gorantla, V. Krishna Rapalli, S. Kumar Dubey, G. Singhvi, Emerging nanoparticulate systems: Preparation techniques and stimuli responsive release characteristics, J. Appl. Pharm. Sci. 9 (2019) 130–143. https://doi.org/10.7324/JAPS.2019.90817.

[7] R.N. Kamble, P.P. Mehta, A. Kumar, Efavirenz Self-Nano-Emulsifying Drug Delivery System: In Vitro and In Vivo Evaluation, AAPS PharmSciTech. 17 (2016) 1240–1247. https://doi.org/10.1208/s12249-015-0446-2.

[8] G. Singhvi, S. Hejmady, V.K. Rapalli, S.K. Dubey, S. Dubey, Nanocarriers for topical delivery in psoriasis, in: R. Shegokar (Ed.), Deliv. Drugs, Elsevier Inc., Germany, 2020: pp. 75–96. https://doi.org/10.1016/b978-0-12-817776-1.00004-3.

[9] T. Waghule, V.K. Rapalli, S. Gorantla, R.N. Saha, S.K. Dubey, A. Puri, G. Singhvi, Nanostructured Lipid Carriers as Potential Drug Delivery Systems for Skin disorders, Curr. Pharm. Des. 26 (2020). https://doi.org/10.2174/1381612826666200614175236.

[10] G. Schett, V.S. Sloan, R.M. Stevens, P. Schafer, Apremilast: A novel PDE4 inhibitor in the treatment of autoimmune and inflammatory diseases, Ther. Adv. Musculoskelet. Dis. 2 (2010) 271–278. https://doi.org/10.1177/1759720X10381432.

[11] H. Yuan, J. Miao, Y.Z. Du, J. You, F.Q. Hu, S. Zeng, Cellular uptake of solid lipid nanoparticles and cytotoxicity of encapsulated paclitaxel in A549 cancer cells, Int. J. Pharm. 348 (2008) 137–145. https://doi.org/10.1016/j.ijpharm.2007.07.012.

[12] S.R. Varma, T.O. Sivaprakasam, A. Mishra, S. Prabhu, M. Rafiq, P. Rangesh, Imiquimod-induced psoriasis-like inflammation in differentiated Human keratinocytes: Its evaluation using curcumin, Eur. J. Pharmacol. 813 (2017) 33–41. https://doi.org/10.1016/j.ejphar.2017.07.040.

[13] J. Sun, Y. Zhao, J. Hu, Curcumin Inhibits Imiquimod-Induced Psoriasis-Like Inflammation by Inhibiting IL-1beta and IL-6 Production in Mice, PLoS One. 8 (2013) e67078. https://doi.org/10.1371/journal.pone.0067078.

[14] N. Shraibom, A. Madaan, V. Joshi, R. Verma, A. Chaudhary, G. Mishra, A. Awasthi, A.T. Singh, M. Jaggi, Evaluation of in vitro Anti-psoriatic Activity of a Novel Polyherbal Formulation by Multiparametric Analysis, Antiinflamm. Antiallergy. Agents Med. Chem. 16 (2017). https://doi.org/10.2174/1871523016666170720160037.

[15] P. R. Varges, C. M. Costa, B. S. Fonseca, M. F. Naccache, P. De Souza Mendes, Rheological Characterization of Carbopol® Dispersions in Water and in Water/Glycerol Solutions, Fluids. 4 (2019) 3. https://doi.org/10.3390/fluids4010003.

[16] C. Gazga-Urioste, E. Rivera-Becerril, G. Pérez-Hernández, N. Angélica Noguez-Méndez, A. Faustino-Vega, C. Tomás Quirino-Barreda, Physicochemical characterization and thermal behavior of hexosomes containing ketoconazole as potential topical antifungal delivery system, Drug Dev. Ind. Pharm. 45 (2019) 168–176. https://doi.org/10.1080/03639045.2018.1526188.

[17] L.Q. Ying, M. Misran, Rheological and physicochemical characterization of alpha-tocopherol loaded lipid nanoparticles in thermoresponsive gel for topical application, Malaysian J. Fundam. Appl. Sci. 13 (2017) 248–252.

https://doi.org/10.11113/mjfas.v13n3.596.

[18] J. Simta, I. Kavita, B. Milind, Novel Long Retentive Posaconazole Ophthalmic Suspension, 6 (2020) 1–10. https://doi.org/10.11648/j.pst.20200401.11.

[19] V. Kakkar, I.P. Kaur, A.P. Kaur, K. Saini, K.K. Singh, Topical delivery of tetrahydrocurcumin lipid nanoparticles effectively inhibits skin inflammation: in vitro and in vivo study, Drug Dev. Ind. Pharm. 44 (2018) 1701–1712. https://doi.org/10.1080/03639045.2018.1492607.

[20] T. Waghule, S. Gorantla, V.K. Rapalli, P. Shah, S.K. Dubey, R.N. Saha, G. Singhvi, Emerging Trends in Topical Delivery of Curcumin Through Lipid Nanocarriers: Effectiveness in Skin Disorders, AAPS PharmSciTech. 21 (2020) 284. https://doi.org/10.1208/s12249-020-01831-9.

[21] N.K. Garg, G. Sharma, B. Singh, P. Nirbhavane, R.K. Tyagi, R. Shukla, O.P. Katare, Quality by Design (QbD)-enabled development of aceclofenac loaded-nano structured lipid carriers (NLCs): An improved dermatokinetic profile for inflammatory disorder(s), Int. J. Pharm. 517 (2017) 413–431. https://doi.org/10.1016/J.IJPHARM.2016.12.010.

[22] S. Jain, R. Addan, V. Kushwah, H. Harde, R.R. Mahajan, Comparative assessment of efficacy and safety potential of multifarious lipid based Tacrolimus loaded nanoformulations, Int. J. Pharm. 562 (2019) 96–104. https://doi.org/10.1016/j.ijpharm.2019.03.042.

[23] M.S. Freag, A.S. Torky, M.M. Nasra, D.A. Abdelmonsif, O.Y. Abdallah, Liquid crystalline nanoreservoir releasing a highly skin-penetrating berberine oleate complex for psoriasis management, Nanomedicine. 14 (2019) 931–954. https://doi.org/10.2217/nnm-2018-0345.

[24] R. Sonawane, H. Harde, M. Katariya, S. Agrawal, S. Jain, Solid lipid nanoparticles-loaded topical gel containing combination drugs: An approach to offset psoriasis, Expert Opin. Drug Deliv. 11 (2014) 1833–1847. https://doi.org/10.1517/17425247.2014.938634.

[25] P.M. Al-Maghrabi, E.S. Khafagy, M.M. Ghorab, S. Gad, Influence of formulation variables on miconazole nitrate–loaded lipid based nanocarrier for topical delivery, Colloids Surfaces B Biointerfaces. 193 (2020) 111046.

https://doi.org/10.1016/j.colsurfb.2020.111046.

[26] J. Sun, W. Dou, Y. Zhao, J. Hu, A comparison of the effects of topical treatment of calcipotriol, camptothecin, clobetasol and tazarotene on an imiquimod-induced psoriasis-like mouse model, Immunopharmacol. Immunotoxicol. 36 (2014) 17–24. https://doi.org/10.3109/08923973.2013.862542.

[27] A. Dadwal, N. Mishra, R.K. Rawal, R.K. Narang, Development and characterisation of clobetasol propionate loaded Squarticles as a lipid nanocarrier for treatment of plaque psoriasis, J. Microencapsul. (2020) 1–14. https://doi.org/10.1080/02652048.2020.1756970.

[28] V.A. Guilherme, L.N.M. Ribeiro, A.C.S. Alcântara, S.R. Castro, G.H. Rodrigues da Silva, C.G. da Silva, M.C. Breitkreitz, J. Clemente-Napimoga, C.G. Macedo, H.B. Abdalla, R. Bonfante, C.M.S. Cereda, E. de Paula, Improved efficacy of naproxen-loaded NLC for temporomandibular joint administration, Sci. Rep. 9 (2019) 1–11. https://doi.org/10.1038/s41598-019-47486-w.

[29] S. Khurana, P.M.S. Bedi, N.K. Jain, Preparation and evaluation of solid lipid nanoparticles based nanogel for dermal delivery of meloxicam, Chem. Phys. Lipids. 175–176 (2013) 65–72. https://doi.org/10.1016/j.chemphyslip.2013.07.010.